Biogeosciences Discuss., 5, 3869–3903, 2008
www.biogeosciences-discuss.net/5/3869/2008/

Biogeosciences Discussions

Biogeosciences Discussions is the access reviewed discussion forum of *Biogeosciences*

Regulation of phytoplankton carbon to chlorophyll ratio by light, nutrients and temperature in the equatorial Pacific Ocean: a basin-scale model

X. J. Wang[1], M. Behrenfeld[2], R. Le Borgne[3], R. Murtugudde[1], and E. Boss[4]

[1]University of Maryland, College Park, MD, USA
[2]Oregon State University, Corvallis, OR, USA
[3]Institut de Recherche pour le Développement, Nouméa Cédex, New Caledonia, France
[4]School of Marine Sciences, University of Maine, Orono, ME, USA

Received: 15 August 2008 – Accepted: 27 August 2008 – Published: 25 September 2008

Correspondence to: X. J. Wang (wwang@essic.umd.edu)

Published by Copernicus Publications on behalf of the European Geosciences Union.

Abstract

The complex effects of light, nutrients and temperature lead to a variable carbon to chlorophyll (C:Chl) ratio in phytoplankton cells. Using field data collected in the equatorial Pacific, we derived a new dynamic model with a non-steady C:Chl ratio as a function of irradiance, nitrate, iron, and temperature. The dynamic model is implemented into a basin-scale ocean circulation-biogeochemistry model and tested in the equatorial Pacific Ocean. The model reproduces well the general features of phytoplankton dynamics in this region. For instance, the simulated deep chlorophyll maximum (DCM) is much deeper in the western warm pool (~100 m) than in the eastern equatorial Pacific (~50 m). The model also shows the ability to reproduce chlorophyll, including not only the zonal, meridional and vertical variations, but also the interannual variability. This study demonstrates that combination of nitrate and iron regulates the spatial and temporal variations in the phytoplankton C:Chl ratio. Particularly, nitrate is responsible for the high C:Chl ratio in the western warm pool while iron is responsible for the frontal features in the C:Chl ratio between the warm pool and the upwelling region. In addition, iron plays a dominant role in regulating the spatial and temporal variations of the C:Chl ratio in the central and eastern equatorial Pacific. While temperature has a relatively small effect on the C:Chl ratio, light is primarily responsible for the vertical decrease of phytoplankton C:Chl ratio in the euphotic zone.

1 Introduction

There is no direct in situ measurement of phytoplankton carbon biomass. Usually, it is estimated from the cell bio-volume through microscopic measurement and flow cytometry (e.g., Ishizaka et al., 1997; Chavez et al., 1996; Brown et al., 2003). This approach is time-consuming, thus cannot be employed routinely in field studies. Alternatively, phytoplankton biomass is often inferred from chlorophyll-*a* (named Chl, hereafter), a pigment that is common to all planktonic autotrophs and can be easily measured. As a

BGD

5, 3869–3903, 2008

result, there has been extensive and growing database of either in situ measurements or remotely sensed Chl. Over the past decade, remotely sensed Chl concentrations have been used for the estimations of the global oceanic primary productivity (Behrenfeld et al., 2005; Behrenfeld and Falkowski, 1997; Carr et al., 2006; Westberry et al., 2008). The extensive Chl database also provides a major reality check on the performance of biogeochemical/ecosystem models (Faure et al., 2006; Armstrong, 2006). However, these approaches rely on realistic conversion between the phytoplankton carbon biomass and Chl concentration.

The relationship between the phytoplankton carbon biomass and Chl concentration is non-linear because of the complex influences by light, nutrients and temperature in the euphotic zone (Armstrong, 2006; Behrenfeld et al., 2002, 2005; Geider et al., 1996, 1997, 1998; Brown et al., 2003; Le Bouteiller et al., 2003). It is well known that the phytoplankton carbon to Chl (C:Chl) ratio decreases from high light to low light under nutrient-replete conditions, a phenomenon called "photoacclimation". The first dynamic model for photoacclimation under nutrient-replete and constant temperature conditions was developed in 1996 (Geider et al., 1996). There have been attempts since to include phytoplanktonic acclimation to nutrients and temperature in the dynamic model development (e.g., Geider et al., 1997, 1998; Behrenfeld et al., 2002; Armstrong, 2006). Most of these approaches are based on laboratory experiments, and prescribe the relationship between the C:Chl ratio and temperature dependence of growth rate because of a lack of observations to parameterize the nutrient dependence. Thus, the combined effects of light, nutrients and temperature on the phytoplankton C:Chl ratio are not well known, and not yet quantified. Phytoplankton dynamic models have been implemented into simple one dimensional biological models (Taylor et al., 1997; Fennel and Boss, 2003; Lefevre et al., 2003; Faugeras et al., 2004; Fujii et al., 2007) and three dimensional regional to global ocean biogeochemical models (Moore et al., 2002; Aumont et al., 2003; Faure et al., 2006). While some of the modeling studies have attempted to simulate a variable C:Chl ratio, there have been limited studies assessing model performance in simulating the phytoplankton C:Chl ratio or

Chl (e.g., Fujii et al., 2007; Faure et al., 2006; Lefevre et al., 2003). Limited studies show significant mismatches between model outputs and observations, including the seasonal to interannual variations of Chl, phytoplankton carbon biomass, and/or C:Chl ratio (e.g., Lefevre et al., 2003). Moreover, little is known about the relative roles of light, temperature and nutrients regulating the large scale variability in the phytoplankton C:Chl ratio. Clearly, studies are needed for both improvement/validation of dynamic models and understanding of mechenimsm underlying the variability of the C:Chl ratio. As Armstrong (2006) pointed out: "the ability to predict phytoplankton growth rates under light and nutrient limitations is fundamental to modeling the ocean carbon cycle, equally fundamental is the ability to predict chlorophyll:carbon ratios, since satellite-based chlorophyll estimates are one of the few data sets to which model output can be compared."

Here, we report an approach of using field data to derive and parameterize the phytoplankton C:Chl ratio as a function of light, temperature, dissolved iron and nitrate, and employing a basin scale 3-dimensional physical-biogeochemical model to test the dynamic model for the equatorial Pacific. The coupled model has demonstrable capability for simulating spatial and temporal variations in physical fields (Murtugudde et al., 1996), ecosystem dynamics, and biogeochemical fields (Wang et al., 2005, 2006a, b). Our approach includes three major parts. First, we use the in situ data collected along 180° during October–November 1996 (Le Borgne and Landry, 2003) to derive a relationship between the phytoplankton C:Chl ratio and regulating factors (i.e., light, nutrients and temperature), and to tune the basin-scale model to match the observations. We then validate the model by using the zonal and meridional distributions of in situ Chl in the upper water column collected from different periods and different locations, and by using the ten years of satellite derived surface Chl. Finally, we carry out a sensitivity study to assess the relative roles of light, nutrients and temperature in regulating the phytoplankton C:Chl ratio for different parts of the equatorial Pacific Ocean.

2 Methodology

2.1 Model description

The ocean general circulation model (OGCM) is a reduced-gravity, primitive-equation, sigma-coordinate model that is coupled to an advective atmospheric mixed layer model (Gent and Cane, 1989; Murtugudde et al., 1996). The model has 20 vertical layers with variable thicknesses. The upper-most layer, the mixed layer, is determined by surface turbulent kinetic energy generation, dynamic instability mixing, and convective mixing to remove static instabilities (Chen et al., 1994). The mixed layer ranges from 10 to 60 m along the equator, and the remaining layers in the euphotic zone (0–120 m) are approximately 10 m in thickness. The model is set up for the Pacific domain between 30° S–30° N with zonal resolution of 1°, and variable meridional resolutions of 0.3–0.6° between 15° S–15° N (1/3° at latitudes <10°), increasing to 2° at the northern and southern boundaries. In the "sponge layer" (10° band) near the boundaries, temperature, salinity, and nitrate are gradually relaxed back towards climatology from the WOA98 atlas (http://www.nodc.noaa.gov/OC5/data_woa.html). The model is forced by climatological monthly means of solar radiation and cloudiness, and 6-day means of surface wind stress from the NCEP/NCAR reanalysis (Kalnay et al., 1996).

The biogeochemical model, modified from an early version (Wang et al., 2006b; Christian et al., 2002), consists of three nutrients (nitrate, ammonium, dissolved iron) and seven biological pools. The biological components include large and small sizes of phytoplankton (P_S and P_L), zooplankton (Z_S and Z_L) and detritus (D_S and D_L), and dissolved organic nitrogen. All biological components are carried in terms of their nitrogen equivalence, except for dissolved iron which is modeled explicitly, using a single Fe:N ratio for all biological compartments except the large phytoplankton. Model structure, equations and biological parameters are given in Wang et al. (2008). The incorporation of iron into the ecosystem model is of vital importance in better predicting the ecosystem response, especially in the equatorial Pacific, because iron has been identified as an important element controlling phytoplankton growth in this region (Martin

BGD
5, 3869–3903, 2008

et al., 1994; Coale et al., 1996). We apply a constant Redfield carbon to nitrogen ratio (6.625) to compute the phytoplankton carbon biomass. Initial conditions are taken from a climatological run, which has been spun up for 30-years with initial conditions from the WOA98 atlas. We perform an interannual run starting from 1987, and use model outputs from the period of 1994–2007.

2.2 Derivation and parameterization of the phytoplankton C:Chl ratio

During the Etude du Broutage en Zone Equatoriale (EBENE) cruise, phytoplankton biomass and chlorophyll concentration were determined from 8° S to 8° N, along 180° during the period of 21 October to 20 November 1996 (Brown et al., 2003). The EBENE data show that the bulk C:Chl ratio in the community varied greatly near the sea surface (79–155 g:g), but was relatively constant (~40 g:g) near the bottom of the euphotic zone. In addition, Le Bouteiller et al. (2003) reports a linear decrease in the phytoplankton C:Chl ratio with depth in the euphotic zone. As shown in Fig. 1, we can predict the C:Chl ratio (η) as a function of depth (Z):

$$\eta = \eta_0 - (\eta_0 - \eta_{\min}) \frac{Z}{Z_E} \quad (1)$$

where η_0 is the C:Chl ratio in the surface, $\eta_{\min}$ the minimum C:Chl ratio at the bottom of the euphotic zone (Z_E). At a given depth Z, light condition can be predicted as:

$$I(z) = I_0 \exp^{-k_A Z} \quad (2)$$

where I_0 is the layer-averaged photosynthetically available radiation (PAR) in the mixed layer. The term k_A, a light attenuation coefficient, is computed as:

$$k_A = k_W + k_C Chl + k_D (D_S + D_L) \quad (3)$$

where k_W, k_C, k_D are the attenuation coefficients for water, chlorophyll and detritus, respectively.

BGD
5, 3869–3903, 2008

By replacing the variable Z by the variable I, we can re-write Eq. (1) as:

$$\eta = \eta_0 - (\eta_0 - \eta_{\min}) \frac{\ln I_0 - \ln I}{\ln I_0 - \ln I_{Z_E}} \quad (4)$$

where I_{Z_E}, the PAR value at the euphotic depth, is 1% of the averaged PAR in the mixed layer (i.e., $I_{Z_E} = 0.01 I_0$). Thus, we can simplify Equation 4 as:

$$\eta = \eta_0 - (\eta_0 - \eta_{\min}) \frac{\ln I_0 - \ln I}{4.605} \quad (5)$$

According to Fig. 8 in Le Bouteiller (2003), there is a linear relationship between the surface C:Chl ratio, η_0, and the growth rate (μ_0^*) under non-light limitation conditions:

$$\eta_0 = \eta_{\max} - k_P \mu_0^* \quad (6)$$

where $\eta_{\max}$ is the maximum C:Chl ratio, and k_P the slope of C:Chl ratio vs. growth rate. There has been other observational evidence that the phytoplankton C:Chl ratio decreases with increased growth rate under non-light limitation (Geider et al., 1997, 1998; Le Bouteiller et al., 2003; Armstrong, 2006; Behrenfeld et al., 2005). The non-light limited growth rate, μ_0^*, can be computed as a function of temperature (T) and the minimum (min) nutrient availability of nitrate (N) and iron (Fe):

$$\mu_0^* = \mu_0 e^{k_T T} \min\left(\frac{NO_3}{K_N + NO_3}, \frac{Fe}{K_{Fe} + Fe}\right) \quad (7)$$

where μ_0 is the maximum growth rate at 0°C, and k_T the temperature dependence coefficient for phytoplankton growth. K_N and K_{Fe} are the half saturation constants for nitrogen and iron limitations on phytoplankton growth, respectively.

There are two phytoplankton categories (large and small) in the model. The small phytoplankton, primarily picophytoplankton (i.e. <2 μm), accounts for >70% of the phytoplankton community determined by total Chl under normal conditions, with larger percentages in the oligotrophic western warm pool than in the mesotrophic High-Nutrient-Low-Chlorophyll (HNLC) region of the equatorial Pacific (Blanchot et al., 2001; Mackey

BGD
5, 3869–3903, 2008

et al., 2002; Le Bouteiller et al., 2003; Le Borgne et al., 2002b). The C:Chl ratio is higher in small phytoplankton cells than in the large ones (Le Bouteiller et al., 2003). Accordingly, we use different physiological parameters for each phytoplankton category (Table 1).

2.3 Model calibration and validation along 180°

Physical and biogeochemical parameters were measured during the EBENE cruise at the end of the 1995–1996 cold phase of the El Niño/ Southern Oscillation (ENSO) (see introduction by Le Borgne and Landry, 2003). The upwelling zone extended west of the Dateline, resulting in relatively high nutrient concentrations in the euphotic zone along 180° (Eldin and Rodier, 2003). Chl concentration reached 0.2 mg m^{-3} near the surface between 5° S and 5° N, and ~0.3 mg m^{-3} at the DCM depth (Brown et al., 2003). Figure 2 shows that our model does a reasonable job in reproducing the observed meridional distributions of temperature, salinity and nitrate in the upper 120 m for the same period (see Figs. 2 and 3 in Eldin and Rodier, 2003). The model is able to simulate the observed meridional variations in the DCM and Chl concentration (Fig. 2b) though the modeled phytoplankton carbon concentrations are lower than the observations (Fig. 2d).

While it is possible to further tune the model to match the observations, we anticipate that potential errors and uncertainties associated with other factors may also contribute to the mis-matches. Field measurements often represent some events occurring at much shorter time scales which can range from less than one hour to several days whereas our model is limited by the shortest frequency of six days (i.e., wind forcing), and model simulations mostly represent mean conditions at much longer time scales (e.g., weeks to months). For example, the EBENE 5-day time series (4–9 November 1996) reveal significant diel variability in the Chl filed. The DCM depth varies from 40 m to 80 m and the Chl concentration ranges from 0.29 mg m^{-3} to 0.38 mg m^{-3} at the DCM (see Fig. 3a in Neveux et al., 2003). Moreover, the EBENE cruise captured many frontal features (including one related to a tropical instability wave) that may not

BGD
5, 3869–3903, 2008

be coherent with the model.

Figure 3 illustrates that the modeled upwelling front is close to the dateline. The modeled Chl, phytoplankton biomass and C:Chl ratio along 175° W show better agreements with the EBENE observations (along 180°) than the modeled values along 180°. For example, the modeled DCM depth varies from ~50 m on the equator to ~100 m off the equator, which is similar to the observations. The model reproduces highest phytoplankton biomass on the equator with a sharp decline over depth. There are some differences in the C:Chl ratio between the model and observation. The model predicts the lowest C:Chl ratio near the equator whereas the observations show the highest C:Chl ratio. As noted by Brown et al. (2003), "the elevated C:Chl ratios in the more productive equatorial zone are somewhat counterintuitive" because high iron near the equator should enhance pigments per cell as seen during the IronEx II fertilization (Landry et al., 2000).

2.4 Satellite and in situ data

There are in situ Chl datasets for both zonal and meridional distributions in the upper water column. Le Borgne et al. (2002a) presented the zonal variations of Chl concentration on the equator during January–February 1991, September–October 1994 and April–May 1996. We compare modeled Chl with the in situ Chl for the last two periods because of the similar spatial coverage (i.e., 165° E–155° W) but for two different phases of the ENSO cycle. September–October 1994 corresponds to the warm phase while April–May 1996 is in the cold phase of the ENSO cycle. It is well known that ENSO is responsible for the large interannual variability in the equatorial Pacific physics and biogeochemistry.

As part of the Equatorial Box Project (http://web.science.oregonstate.edu/ocean.productivity/box.php), water samples were collected during the Tropical Atmosphere Ocean (TAO) cruises along 140° W and 125° W during 2005–2007. Surface particulate organic carbon (POC) concentrations were measured by collecting water samples at 3 m using the flow-through seawater system. Chl concentrations were determined us-

ing a Turner fluorometer and by HPLC. Technical details can be found in Behrenfeld and Boss (2006). The in situ Chl and POC data can be accessed at the project website. We use these data for further model validations, focusing on meridional variations in the eastern equatorial Pacific.

There is a continuous record of high-quality ocean color data from the Sea-viewing Wide Field-of-view Sensor (SeaWiFS) going back to September 1997. The satellite derived Chl provides spatial distributions and temporal variations, which are useful for validation of the modeled surface Chl at large scales.

3 Results and discussion

3.1 Model-data comparisons

3.1.1 Along 140° W and 125° W

Here, we use in situ data collected along 125° W and 140° W during 2005–2007 to evaluate the model skills in predicting meridional distribution of Chl in the eastern equatorial Pacific. Figures 4–6 show that the model reproduces some observed features, particularly the meridional distribution of Chl. For the period of September 2005 (Fig. 4), the in situ Chl concentration (0.2–0.5 mg m^{-3}) is slightly higher than the modeled Chl (0.1–0.4 mg m^{-3}) in the upper euphotic zone along 125° W. Along 140° W, the modeled Chl shows a similar range to the in situ Chl in the upper euphotic zone. Both in situ and modeled Chl concentrations are considerably higher than the SeaWiFS Chl on the equator.

Chl concentration is lower during September 2006 (0.1–0.3 mg m^{-3}, Fig. 5) than during September 2005 (Fig. 4) particularly along 140° W. While the model over-estimates Chl concentration in the upper euphotic zone on the equator along 140° W, modeled Chl agrees well with the in situ measurements along 125° W during September 2006 (Fig. 5f). For the period of May 2007 (Fig. 6), both in situ data and model simulation

show stronger DCM, compared with those during September 2005 and September 2006. In general, there is a considerable difference in the surface Chl concentration among the in situ, modeled and the SeaWiFS data. The SeaWiFS Chl concentration is generally lower with a weaker meridional variation than the in situ surface Chl. The modeled surface Chl shows better agreements with the in situ surface Chl than with the SeaWiFS Chl. The in situ Chl concentrations reach 0.5 mg m^{-3} at the DCM during 2005–2007, which are considerably higher than those in earlier studies (Brown et al., 2003; Le Borgne et al., 2002a).

While there is a lack of in situ measurements of phytoplankton carbon biomass for model validation, the in situ surface POC can be used to check the model performance. Figure 7 shows the comparisons between the in situ surface POC and the modeled POC in the mixed layer. Overall, the model reproduces the meridional distribution of surface POC, reasonably well, showing moderate increase (by less than a factor of two) from off the equator to the equator. Both the in situ data and model simulation reveal relatively higher surface POC concentrations to the north than to the south during May 2007.

3.1.2 Zonal variations

There are two distinct regions in the equatorial Pacific: the warm pool to the west, and the upwelling region in the central and eastern Pacific (Picaut et al., 2001; Le Borgne et al., 2002a). The warm pool has deeper thermocline and nutricline, with low nutrient concentrations in the mixed layer. In contrast, surface nutrient concentrations are higher in the upwelling region. Observations (Le Borgne et al., 2002a) indicate that surface Chl concentration is less than 0.1 mg m^{-3} in the warm pool, and approximately 0.2 mg m^{-3} in the upwelling region. The DCM is placed at ~100 m in the western warm pool and at ~50 m in the central and eastern equatorial Pacific. Figure 8 shows that the model reproduces many observed features in the distributions of the upper water column Chl. For instance, the surface Chl concentration to the west of 170° W is <0.1 mg m^{-3} during October 1994, but approximately 0.2 mg m^{-3} during April–May

BGD
5, 3869–3903, 2008

1996. Both in situ data and model simulation show relatively flat DCM during the period of April–May 1996, but deeper DCM in the western warm pool (~90 m) than in the central equatorial Pacific (~50 m) during October 1994.

3.1.3 Modeled surface Chl vs. the SeaWiFS derived Chl

The equatorial Pacific is known to undergo significant changes in physical and biogeochemical properties at seasonal to interannual time-scales. There is a warm season (March–May) in association with large solar warming and weak wind mixing (Cronin and Kessler, 2002), and an upwelling season associated with strong winds in boreal fall. The interannual variations in physical and biogeochemical fields largely correspond with the ENSO cycle (Wang et al., 2005, 2006a, b; Feely et al., 2002; Le Borgne et al., 2002a). In this section, we compare modeled Chl with the SeaWiFS data for the period of 1997–2007. In order to understand how the ENSO phenomenon affects the interannual variability of surface Chl, we introduce an annual mean longitude of the front between the HNLC and warm pool, which is estimated from the SOI: 173.2–10.75 SOI (Le Borgne et al., 2002a). The SOI values are annual means of the standardized data of Tahiti minus Darwin sea-level pressures from the Climate Prediction Centre (http://www.cpc.ncep.noaa.gov/data/indices/soi).

Figure 9 shows that the model simulation captures many observed features in the SeaWiFS Chl, including the magnitude, and the spatial and temporal variations. Simulated Chl concentrations in the surface water range from ~0.1 mg m^{-3} in the warm pool to ~0.2 mg m^{-3} in the HNLC region, which is consistent with the SeaWiFS derived Chl. The model reproduces the extremely low Chl in the central equatorial Pacific during the warm phases of 1997/1998, 2002 and 2006 ENSO events. However, the model under-estimates Chl concentration during the cold phase of 1998 ENSO, which could be related to the overall weak amplitude of the NCEP winds (Hackert et al., 2001). There is also a mis-match in the eastern equatorial Pacific between the model and the SeaWiFS data. While the SeaWiFS data under-estimate the surface Chl concentration (Figs. 4–6), the model may not be able to reproduce the spatial and temporal variability

BGD
5, 3869–3903, 2008

at small scales due to model deficiency in physical field (e.g., seasonality in the eastern equatorial Pacific, Wang et al., 2006a), in association with the standard cold-bias in most state of the art models (see Murtugudde et al., 2002). Nevertheless, the model reproduces well the seasonal Chl (e.g., peak in boreal spring) in the western warm pool, and interannual variability for the HNLC front.

3.2 Relative role of nutrients and temperature

The combined effects of light, nutrients and temperature on the phytoplankton C:Chl ratio has been a complicated issue. The photoacclimation phenomenon, i.e., low irradiance leading to low C:Chl ratio, is well known (Geider et al., 1996, 1997, 1998; Armstrong, 2006; Behrenfeld et al., 2005). However, little is known about the relative role of nutrients and temperature on the phytoplankton C:Chl ratio. To address this issue, we carry out a sensitivity study consisting of a standard simulation and four other simulations (Table 2). For the standard simulation, we keep SST, iron and nitrate concentrations variable in Eq. (7). For the other simulations, we apply one or two constants that are the averaged values of SST, surface iron or/and nitrate concentrations calculated from the standard simulation for the year 1994. We then compare simulated C:Chl ratio with that from the standard simulation for the period of September–October 1994. We choose this period because it has in situ Chl data for model validation, and the year 1994 is close to an average year with a slightly negative SOI.

Figure 10 shows simulated Chl, phytoplankton biomass and C:Chl ratio from the standard simulation. Modeled surface Chl concentration is less than 0.1 mg m^{-3} in the warm pool and ~0.25 mg m^{-3} in the HNLC area. Chl concentration at the DCM displays a small range (0.2–0.3 mg m^{-3}) in both the western warm pool and the central equatorial Pacific. Modeled DCM depth is much deeper in the warm pool (~100 m) than in the HNLC region (~50 m). These values agree well with those measured during boreal fall 1994 in the equatorial Pacific (Le Borgne et al., 2002a, b). The phytoplankton C:Chl ratio co-varies with nitrate, iron and temperature, showing higher values in the western warm pool than in the HNLC region.

SST is high year around in the equatorial Pacific, varying from 22°C in the eastern upwelling region to ~30°C in the warm pool. Replacing the variable SST in Eq. (7) with a constant results in little change in model simulations of the zonal and meridional variations of the phytoplankton C:Chl ratio (Fig. 11a and b), indicating that temperature has little effect on the C:Chl ratio in the equatorial Pacific. Applying a constant iron concentration causes moderate changes in the phytoplankton C:Chl ratio (Fig. 11c and d). The model considerably under-estimates the C:Chl ratio near the front between the warm pool and the HNLC waters (i.e., 180°–160° W) and on the equator in the warm pool. Eliminating nitrate effect results in large changes in the magnitude and meridional variability of the phytoplankton C:Chl ratio in the warm pool (Fig. 11e and f). However, nitrate shows little effect on the phytoplankton dynamics in the area east of 160° W. These results suggest that nitrate is the primary factor regulating the phytoplankton C:Chl ratio in the western warm pool whereas iron plays an important role in the HNLC area, and particularly near its western boundary. These two limitations, nitrate in the oligotrophic warm pool and iron in the mesotrophic HNLC region, have been characterized in the equatorial Pacific (Le Borgne et al., 2002b). Apparently, eliminating both nitrate and iron effects produces little zonal and meridional variability in the phytoplankton C:Chl ratio, leading to even higher bias in the warm pool Chl (Fig. 11g and h).

Statistical analyses are applied to the model outputs to quantify the effects of the variability in the SST, iron and nitrate on the phytoplankton C:Chl ratio. Three regions are examined: the warm pool (160° E–180°, 5° N–5° S), the frontal region (180°–160° W, 5° N–5° S), and the central equatorial Pacific (160° W–140° W, 5° N–5° S). Three criteria are used to assess the sensitivity of the C:Chl ratio (referring as X). The first one is the bias which is the difference of the averages ($\overline{X}$) between an experiment (s) and the standard simulation (c). The second is the correlation (r) between the two simulations. The last is the ratio of the variance from an experiment to the variance

from the standard simulation:

$$Vs/Vc = \frac{\frac{1}{n}\sum_{1}^{n}(Xs - \overline{X}s)^2}{\frac{1}{n}\sum_{1}^{n}(Xc - \overline{X}c)^2} \quad (8)$$

where n is the number of the values for each experiment. A best match between an experiment and the standard simulation, i.e. indications of closest to zero for the bias, and closest to one for both the r and the Vs/Vc ratio, suggests that the tested variable has the smallest influence out of all the variables on the phytoplankton C:Chl ratio. Conversely, the bigger the mismatch, the larger the effect of the tested variable has.

Table 3 shows that the avaraged C:Chl ratio and statistics at 20 m and 60 m. Apparently, the SSTM experiment reveals the best match in the warm pool and the frontal region, and the NO_3M in the HNLC region. In addition, the SSTM produce zero bias, high correlation (r=0.993–0.994) and almost perfect Vs/Vc ratio (1.13–1.16) in the HNLC region. These analyses indicate that temperature has little effect on the phytoplankton C:Chl ratio in the entire equatorial Pacific, and nitrate in the HNLC region. While model experiments clearly show a dominant role of iron in regulating the phytoplankton C:Chl ratio in the HNLC region, changes in the C:Chl ratio induced by iron are relatively small (~5%), indicating a rather stable ecosystem under the HNLC conditions (Le Borgne et al., 2002a; Le Borgne and Landry, 2003).

For the warm pool, the FeM simulates much smaller bias and higher correlation (r>0.96) than the NO_3M, suggesting that nitrate plays a larger role in determining the phytoplankton C:Chl ratio than iron. However, the Vs/Vc is close to one in the NO_3M, which indicates nitrate has little effect on the spatial variability though it regulates the magnitude of the C:Chl ratio in the warm pool. Interestingly, removing both nitrate and iron effects (i.e., the $FeNO_3$M) produces much larger bias, lower correlation and smaller Vs/Vc than only eliminating nitrate (i.e., the NO_3M), reflecting complex interaction of nitrate and iron limitations west of the dateline (Behrenfeld et al., 2006).

BGD
5, 3869–3903, 2008

In the frontal region, the model simulates larger bias in the FeM (>20%) than in the NO_3M (<10%), which indicates relatively larger effect of iron on the phytoplankton C:Chl ratio than nitrate. But both the correlation and Vs/Vc are slightly closer to one in the FeM than in the NO_3M, suggesting that nitrate may play a certain role in regulation of the spatial varibility of C:Chl ratio. Clearly, the interaction of iron and nitrate is weaker in the frontal region than in the warm pool.

4 Summary and conclusions

We have carried out a basin-scale modeling study of phytoplankton dynamics, and explored the regulation of light, iron, nitrate and temerature with a non-steady C:Chl ratio in the equatorial Pacific. While there are limited data of the phytoplankton C:Chl ratio in this region, there is a considerable amount of in situ Chl data for the upper water column with reasonably good spatial and temporal coverage in addition to the surface Chl derived from the SeaWiFS imagery. Our model reproduces well the general features of phytoplankton dynamics in this region, including not only the zonal, meridional and vertical variations, but also the interannual variability of Chl concentration. The large spatio-temporal contrasts in physical and biogeochemical fields in the equatorial Pacific make this region an ideal test bed for exploring the regulation of light, nutrients and temperature on the phytoplankton C:Chl ratio. We have demonstrated the applicability of the new C:Chl dynamic model. Our study indicates that nitrate and iron together regulate the zonal and meridional variations in the C:Chl ratio thus Chl dynamics in the equatorial Pacific. Nitrate is responsible for the high C:Chl ratio in the western warm pool while iron determines the displacement of the HNLC front. Light is primarily responsible for the vertical decrease of phytoplankton C:Chl ratio. Temperature has a relatively small effect on the C:Chl ratio in the equatorial Pacific.

Acknowledgements. This research is supported by National Aeronautics and Space Administration (NASA). We thank NASA for providing SeaWiFS derived Chl data. We thank J. Arrington for the in situ POC and Chl measurements. We appreciate the constructive comments of

A. Gnanadesikan on the model sensitivity study.

References

Armstrong, R. A.: Optimality-based modeling of nitrogen allocation and photoacclimation in photosynthesis, Deep-Sea Res. Pt. II, 53, 513–531, 2006.

Aumont, O., Maier-Reimer, E., Blain, S., and Monfray, P.: An ecosystem model of the global ocean including Fe, Si, P colimitations, Global Biogeochem. Cy., 17, 1060, doi:10.1029/2001GB001745, 2003.

Behrenfeld, M. J. and Falkowski, P. G.: Photosynthetic rates derived from satellite-based chlorophyll concentration, Limnol. Oceanogr., 42, 1–20, 1997.

Behrenfeld, M. J., Maranon, E., Siegel, D. A., and Hooker, S. B.: Photoacclimation and nutrient-based model of light-saturated photosynthesis for quantifying oceanic primary production, Mar. Ecol.-Prog. Ser., 228, 103–117, 2002.

Behrenfeld, M. J., Boss, E., Siegel, D. A., and Shea, D. M.: Carbon-based ocean productivity and phytoplankton physiology from space, Global Biogeochem. Cy., 19, GB1006, doi:10.1029/2004GB002299, 2005.

Behrenfeld, M. J. and Boss, E.: Beam attenuation and chlorophyll concentration as alternative optical indices of phytoplankton biomass, J. Mar. Res., 64, 431–451, 2006.

Behrenfeld, M. J., Worthington, K., Sherrell, R. M., Chavez, F. P., Strutton, P., McPhaden, M., and Shea, D. M.: Controls on tropical Pacific Ocean productivity revealed through nutrient stress diagnostics, Nature, 442, 1025–1028, 2006.

Blanchot, J., Andre, J. M., Navarette, C., Neveux, J., and Radenac, M. H.: Picophytoplankton in the equatorial Pacific: vertical distributions in the warm pool and in the high nutrient low chlorophyll conditions, Deep-Sea Res. Pt. I, 48, 297–314, 2001.

Brown, S. L., Landry, M. R., Neveux, J., and Dupouy, C.: Microbial community abundance and biomass along a 180 degrees transect in the equatorial Pacific during an El Nino-Southern Oscillation cold phase, J. Geophys. Res., 108, 8139, doi:10.1029/2001JC000817, 2003.

Carr, M.-E., Friedrichs, M. A. M., Schmeltz, M., Noguchi Aita, M., Antoine, D., Arrigo, K. R., Asanuma, I., Aumont, O., Barber, R., and Behrenfeld, M.: A comparison of global estimates of marine primary production from ocean color, Deep-Sea Res. Pt. II, 53, 741–770, 2006.

Chavez, F. P., Buck, K. R., Service, S. K., Newton, J., and Barber, R. T.: Phytoplankton variability in the central and eastern tropical Pacific, Deep-Sea Res. Pt. II, 43, 835–870, 1996.
Chen, D., Rothstein, L. M., and Busalacchi, A. J.: A hybrid vertical mixing scheme and its application to tropical ocean models, J. Phys. Oceanogr., 24, 2156–2179, 1994.
Christian, J. R., Verschell, M. A., Murtugudde, R., Busalacchi, A. J., and McClain, C. R.: Biogeochemical modelling of the tropical Pacific Ocean. I: Seasonal and interannual variability, Deep-Sea Res. Pt. II, 49, 509–543, 2002.
Coale, K. H., Fitzwater, S. E., Gordon, R. M., Johnson, K. S., and Barber, R. T.: Control of community growth and export production by upwelled iron in the equatorial Pacific Ocean, Nature, 379, 621–624, 1996.
Cronin, M. F. and Kessler, W. S.: Seasonal and interannual modulation of mixed layer variability at 0 degrees, 110 degrees W, Deep-Sea Res. Pt. I, 49, 1–17, 2002.
Eldin, G. and Rodier, M.: Ocean physics and nutrient fields along 180 degrees during an El Nino-Southern Oscillation cold phase, J. Geophys. Res., 108, 8137, doi:10.1029/2000JC000746, 2003.
Faugeras, B., Bernard, O., Sciandra, A., and Lévy, M.: A mechanistic modelling and data assimilation approach to estimate the carbon/chlorophyll and carbon/nitrogen ratios in a coupled hydrodynamical-biological model, Nonlin. Processes Geophys., 11, 515–533, 2004, http://www.nonlin-processes-geophys.net/11/515/2004/.
Faure, V., Pinazo, C., Torreton, J. P., and Douillet, P.: Relevance of various formulations of phytoplankton chlorophyll a : carbon ratio in a 3D marine ecosystem model, Comptes Rendus Biologies, 329, 813–822, 10.1016/crvi.2006.07.006/ISSN 1631-0691, 2006.
Feely, R. A., Boutin, J., Cosca, C. E., Dandonneau, Y., Etcheto, J., Inoue, H. Y., Ishii, M., Quere, C. L., Mackey, D. J., and McPhaden, M.: Seasonal and interannual variability of CO_2 in the equatorial Pacific, Deep-Sea Res. Pt. II, 49, 2443–2469, 2002.
Fennel, K. and Boss, E.: Subsurface maxima of phytoplankton and chlorophyll: Steady-state solutions from a simple model, Limnol. Oceanogr., 48, 1521–1534, 2003.
Fujii, M., Boss, E., and Chai, F.: The value of adding optics to ecosystem models: a case study, Biogeosciences, 4, 817–835, 2007, http://www.biogeosciences.net/4/817/2007/.
Geider, R. J., Macintyre, H. L., and Kana, T. M.: A dynamic model of photoadaptation in phytoplankton, Limnol. Oceanogr., 41, 1–15, 1996.
Geider, R. J., MacIntyre, H. L., and Kana, T. M.: Dynamic model of phytoplankton growth and

acclimation: responses of the balanced growth rate and the chlorophyll a:carbon ratio to light, nutrient-limitation and temperature, Mar. Ecol.-Prog. Ser., 148, 187–200, 1997.
Geider, R. J., Macintyre, H. L., and Kana, T. M.: A dynamic regulatory model of phytoplanktonic acclimation to light, nutrients, and temperature, Limnol. Oceanogr., 43, 679–694, 1998.
Gent, P. R. and Cane, M. A.: A reduced gravity, primitive equation model of the upper Equatorial Ocean, J. Comput. Phys., 81, 444–480, 1989.
Hackert, E. C., Busalacchi, A. J., and Murtugudde, R.: A wind comparison study using an ocean general circulation model for the 1999–1998 El Nino, J. Geophys. Res., 106, 2345–2362, 2001.
Ishizaka, J., Harada, K., Ishikawa, K., Kiyosawa, H., Furusawa, H., Watanabe, Y., Ishida, H., Suzuki, K., Handa, N., and Takahashi, M.: Size and taxonomic plankton community structure and carbon flow at the equator, 175° E during 1990–1994, Deep-Sea Res. Pt. II, 44, 1927–1949, 1997.
Kalnay, E., Kanamitsu, M., Kistler, R., Collins, W., Deaven, D., Gandin, L., Iredell, M., Saha, S., White, G., Woollen, J., Zhu, Y., Chelliah, M., Ebisuzaki, W., Higgins, W., Janowiak, J., Mo, K. C., Ropelewski, C., Wang, J., Leetmaa, A., Reynolds, R., Jenne, R., and Joseph, D.: The NCEP/NCAR 40-year reanalysis project, B. Am. Meteorol. Soc., 77, 437–471, 1996.
Landry, M. R., Ondrusek, M. E., Tanner, S. J., Brown, S. L., Constantinou, J., Bidigare, R. R., Coale, K. H., and Fitzwater, S.: Biological response to iron fertilization in the eastern equatorial Pacific (IronEx II). I. Microplankton community abundances and biomass, Mar. Ecol.-Prog. Ser., 201, 27–42, 2000.
Le Borgne, R., Barber, R. T., Delcroix, T., Inoue, H. Y., Mackey, D. J., and Rodier, M.: Pacific warm pool and divergence: temporal and zonal variations on the equator and their effects on the biological pump, Deep-Sea Res. Pt. II, 49, 2471–2512, 2002a.
Le Borgne, R., Feely, R. A., and Mackey, D. J.: Carbon fluxes in the equatorial Pacific: a synthesis of the JGOFS programme, Deep-Sea Res. Pt. II, 49, 2425–2442, 2002b.
Le Borgne, R. and Landry, M. R.: EBENE: A JGOFS investigation of plankton variability and trophic interactions in the equatorial Pacific (180 degrees), J. Geophys. Res., 108, 8136, doi:10.1029/2001JC001252, 2003.
Le Bouteiller, A., Leynaert, A., Landry, M. R., Le Borgne, R., Neveux, J., Rodier, M., Blanchot, J., and Brown, S. L.: Primary production, new production, and growth rate in the equatorial Pacific: Changes from mesotrophic to oligotrophic regime, J. Geophys. Res., 108, 8141, doi:10.1029/2001JC000914, 2003.

Lefevre, N., Taylor, A. H., Gilbert, F. J., and Geider, R. J.: Modeling carbon to nitrogen and carbon to chlorophyll a ratios in the ocean at low latitudes: Evaluation of the role of physiological plasticity, Limnol. Oceanogr., 48, 1796–1807, 2003.

Mackey, D. J., Blanchot, J., Higgins, H. W., and Neveux, J.: Phytoplankton abundances and community structure in the equatorial Pacific, Deep-Sea Res. Pt. II, 49, 2561–2582, 2002.

Martin, J. H., Coale, K. H., Johnson, K. S., Fitzwater, S. E., Gordon, R. M., Tanner, S. J., Hunter, C. N., Elrod, V. A., Barber, R. T., Lindley, S., Watson, A. J., and Van Scoy, K.: Testing the iron hypothesis in ecosystems of the equatorial Pacific Ocean, Nature, 371, 123–129, 1994.

Moore, J. K., Doney, S. C., Kleypas, J. A., Glover, D. M., and Fung, I. Y.: An intermediate complexity marine ecosystem model for the global domain, Deep-Sea Res. Pt. II, 49, 403–462, 2002.

Murtugudde, R., Seager, R., and Busalacchi, A.: Simulation of the tropical oceans with an ocean GCM coupled to an atmospheric mixed-layer model, J. Climate, 9, 1795–1815, 1996.

Murtugudde, R., Beauchamp, J., McClain, C. R., Lewis, M., and Busalacchi, A. J.: Effects of penetrative radiation on the upper tropical ocean circulation, J. Climate, 15, 470–486, 2002.

Neveux, J., Dupouy, C., Blanchot, J., Le Bouteiller, A., Landry, M. R., and Brown, S. L.: Diel dynamics of chlorophylls in high-nutrient, low-chlorophyll waters of the equatorial Pacific (180 degrees): Interactions of growth, grazing, physiological responses, and mixing, J. Geophys. Res.-Oceans, 108, 8140, doi:10.1029/2000JC000747, 2003.

Picaut, J., Ioualalen, M., Delcroix, T., Masia, F., Murtugudde, R., and Vialard, J.: The oceanic zone of convergence on the eastern edge of the Pacific warm pool: A synthesis of results and implications for El Nino-Southern Oscillation and biogeochemical phenomena, J. Geophys. Res., 106, 2363–2386, 2001.

Taylor, A. H., Geider, R. J., and Gilbert, F. J. H.: Seasonal and latitudinal dependencies of phytoplankton carbon-to-chlorophyll a ratios: Results of a modelling study, Mar. Ecol.-Prog. Ser., 152, 51–66, 1997.

Wang, X. J., Christian, J., Murtugudde, R., and Busalacchi, A.: Ecosystem dynamics and export production in the central and eastern equatorial Pacific: a modeling study of impact of ENSO, Geophys. Res. Lett., 32, L02608, doi:10.1029/2004GL021538, 2005.

Wang, X. J., Christian, J. R., Murtugudde, R., and Busalacchi, A. J.: Spatial and temporal variability of the surface water pCO_2 and air-sea CO_2 flux in the equatorial Pacific during 1980–2003: a basin-scale carbon model, J. Geophys. Res., 111, C07S04, doi:10.1029/2005JC002972, 2006a.

Wang, X. J., Christian, J. R., Murtugudde, R., and Busalacchi, A. J.: Spatial and temporal variability in new production in the equatorial Pacific during 1980–2003: Physical and biogeochemical controls, Deep-Sea Res. Pt. II, 53, 677–697, 2006b.

Wang, X. J., Le Borgne, R., Murtugudde, R., Busalacchi, A. J., and Behrenfeld, M.: Spatial and temporal variations in dissolved and particulate organic nitrogen in the equatorial Pacific: biological regulations and physical influences, Biogeosciences Discuss., 5, 3267–3305, 2008, http://www.biogeosciences-discuss.net/5/3267/2008/.

Westberry, T., Behrenfeld, M. J., Siegel, D. A., and Boss, E.: Carbon-based primary productivity modeling with vertically resolved photoacclimation, Global Biogeochem. Cy., 22, GB2024, doi:10.1029/2007gb003078, 2008.

Table 1. Biological parameters used for small and large phytoplankton.

Parameter	Symbol	Unit	Small	Large
Maximum growth rate at 0°C	μ_{S0}	d^{-1}	0.58	1.16
Temp. dependent coefficient for μ	k_T	$^{\circ}C^{-1}$	0.06	0.06
Half saturation constant for N limitation	K_N	nmol m^{-3}	0.2	0.6
Half saturation constant for iron limitation	K_{Fe}	nmol m^{-3}	14	150
Minimum C:Chl ratio	η_{min}	g:g	30	15
Maximum C:Chl ratio	η_{max}	g:g	200	120
Photoacclimation coefficient	k_P	(g:g) d	95	70
Light attenuation constant for water	k_W	m^{-1}	0.028	
Light attenuation constant for chlorophyll	k_C	m^{-1} (mg chl $m^{-3})^{-1}$	0.058	
Light attenuation constant for detritus	k_D	m^{-1}(mmol N $m^{-3})^{-1}$	0.008	

Table 2. Model experiments with different combinations of variables in Eq. (7).

Experiment	SST (°C)	Nitrate ($mmol\,m^{-3}$)	Iron ($nmol\,m^{-3}$)
Standard	Variable	Variable	Variable
SSTM	26.9	Variable	Variable
FeM	Variable	Variable	18.9
NO_3M	Variable	4	Variable
$FeNO_3M$	Variable	4	18.9

Table 3. Statistics of C/Chl ratio in the surface (20 m) and subsurface (60 m) in different regions.

Experiment	20 m Value	Bias	Correlation	Vs/Vc	60 m Value	Bias	Correlation	Vs/Vc
160° E–180°, 5° N–5° S								
(1) Standard	186				134			
(2) SSTM	188	2	0.998	0.70	135	1	0.996	0.78
(3) FeM	179	−7	0.985	3.09	129	−5	0.968	2.45
(4) NO_3M	113	−73	0.683	1.60	82	−52	0.676	1.01
(5) $FeNO_3M$	94	−92	0.387	0.01	70	−64	0.438	0.08
180°–160° W, 5° N–5° S								
(1) Standard	141				100			
(2) SSTM	147	6	0.991	1.06	104	4	0.994	1.04
(3) FeM	105	−35	0.856	1.48	76	−23	0.894	1.49
(4) NO_3M	130	−11	0.731	0.50	91	−9	0.726	0.41
(5) $FeNO_3M$	94	−47	0.680	0.01	67	−32	0.438	0.08
160° W–140° W, 5° N–5° S								
(1) Standard	97				67			
(2) SSTM	97	0	0.993	1.16	67	0	0.994	1.13
(3) FeM	92	−5	0.606	0.07	63	−4	0.709	0.20
(4) NO_3M	96	−1	0.994	0.86	67	0	0.994	0.92
(5) $FeNO_3M$	92	−5	0.650	0.07	63	−4	0.705	0.21

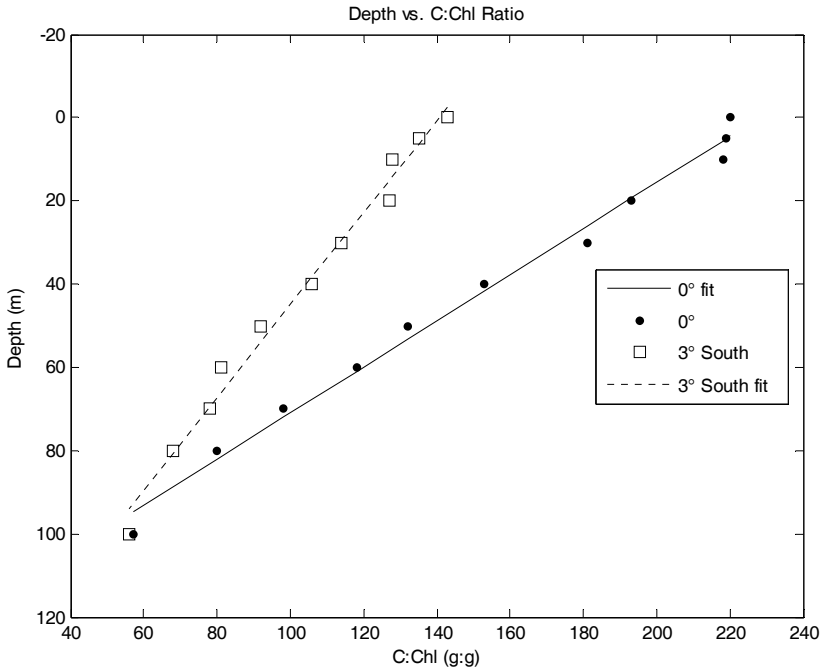

Fig. 1. Measured vertical distribution of community C:Chl ratio at 0° and 3° S along 180° during October–November 1996. Data are from the Table 6 in Le Bouteiller et al. (2003).

BGD
5, 3869–3903, 2008

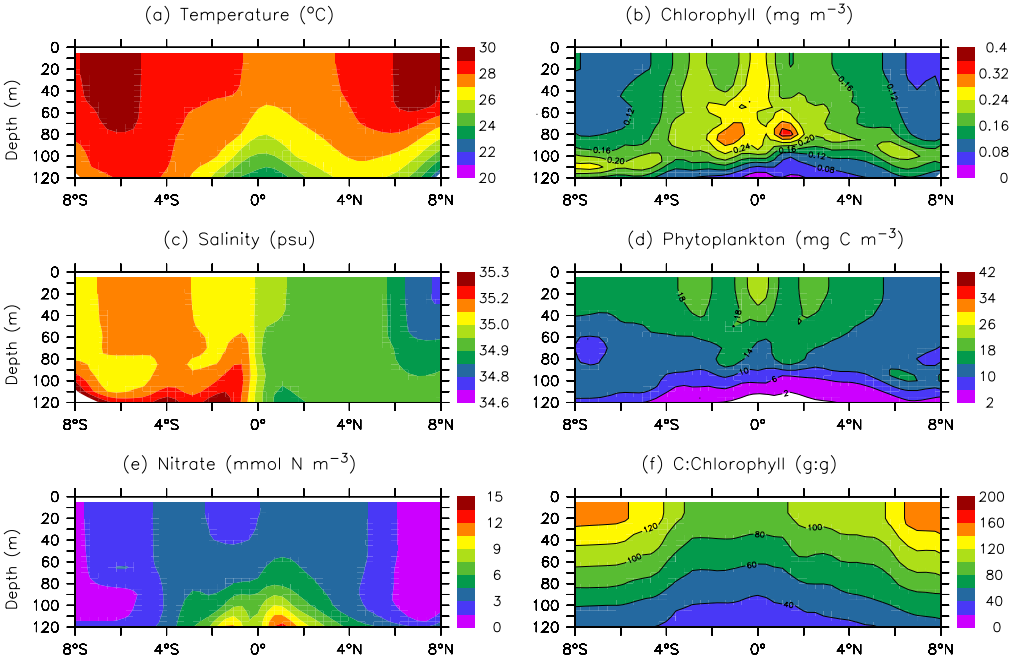

Fig. 2. Modeled profiles of **(a)** temperature, **(b)** chlorophyll, **(c)** salinity, **(d)** phytoplankton biomass, **(e)** nitrate, and **(f)** C:Chl ratio along 180° during October–November 1996.

BGD
5, 3869–3903, 2008

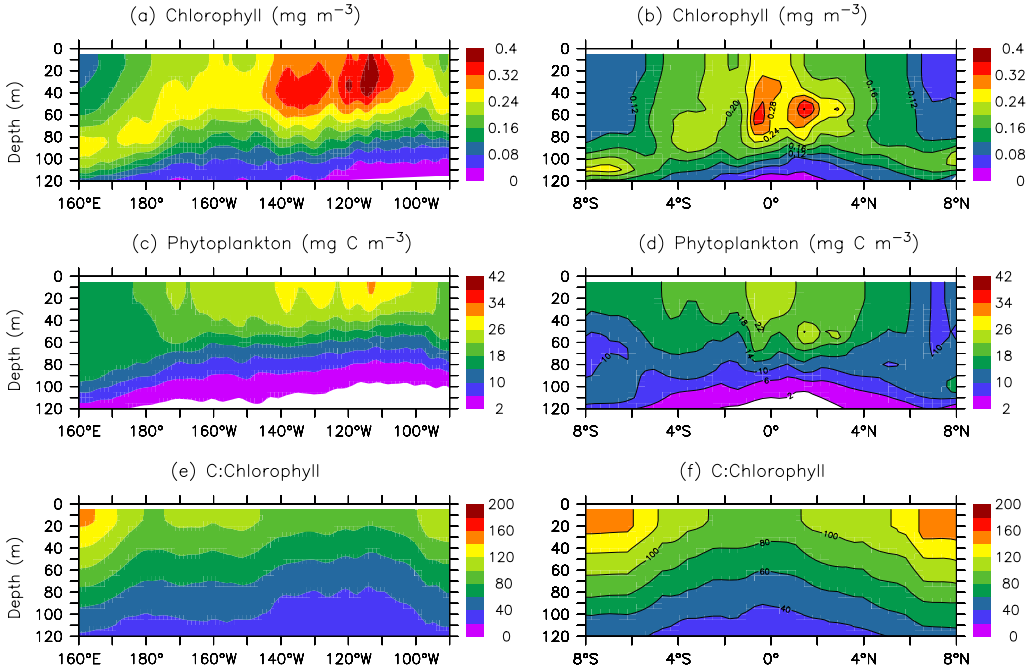

Fig. 3. Modeled zonal (left panel, 2° N–2° S) and meridional (along 175° W) distributions of **(a)** and **(b)** chlorophyll, **(c)** and **(d)** phytoplankton biomass, and **(e)** and **(f)** C:Chl ratio during October–November 1996.

BGD
5, 3869–3903, 2008

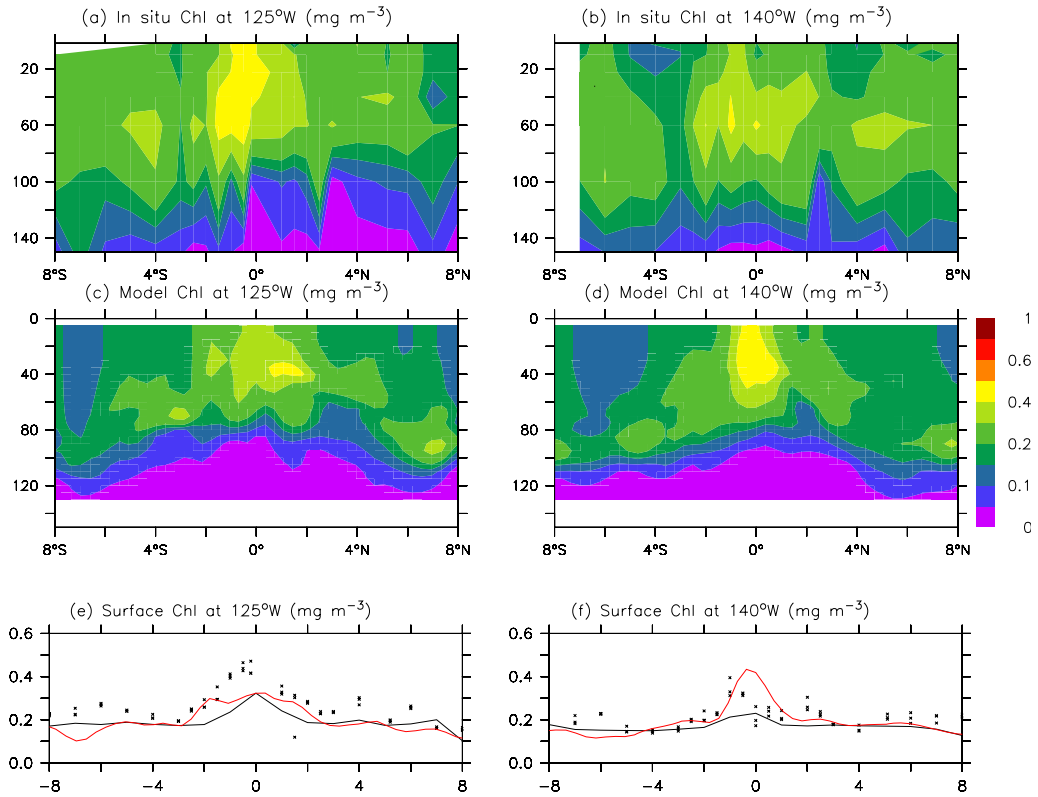

Fig. 4. SeaWiFS, in situ and modeled chlorophyll during September 2005. In situ chlorophyll **(a)** along 125° W and **(b)** along 140° W, and modeled chlorophyll **(c)** along 125° W and **(d)** along 140° W, and surface (0–20 m) chlorophyll concentrations **(e)** along 125° W and **(f)** along 140° W from in situ (symbols), model (red lines) and SeaWiFS (black lines).

BGD
5, 3869–3903, 2008

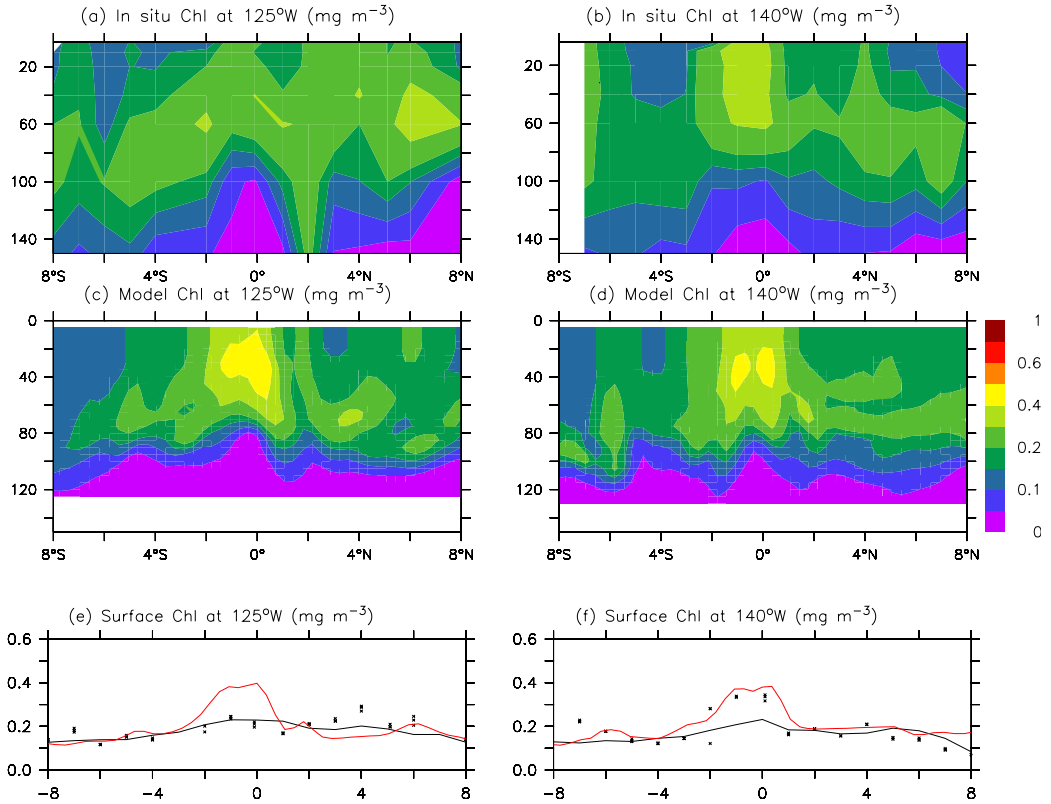

Fig. 5. SeaWiFS (September 2006), in situ (24 August–19 September 2006) and modeled (September 2006) chlorophyll. In situ chlorophyll **(a)** along 125° W and **(b)** along 140° W, and modeled chlorophyll **(c)** along 125° W and **(d)** along 140° W, and surface (0–20 m) chlorophyll concentrations **(e)** along 125° W and **(f)** along 140° W from in situ (symbols), model (red lines) and SeaWiFS (black lines).

BGD
5, 3869–3903, 2008

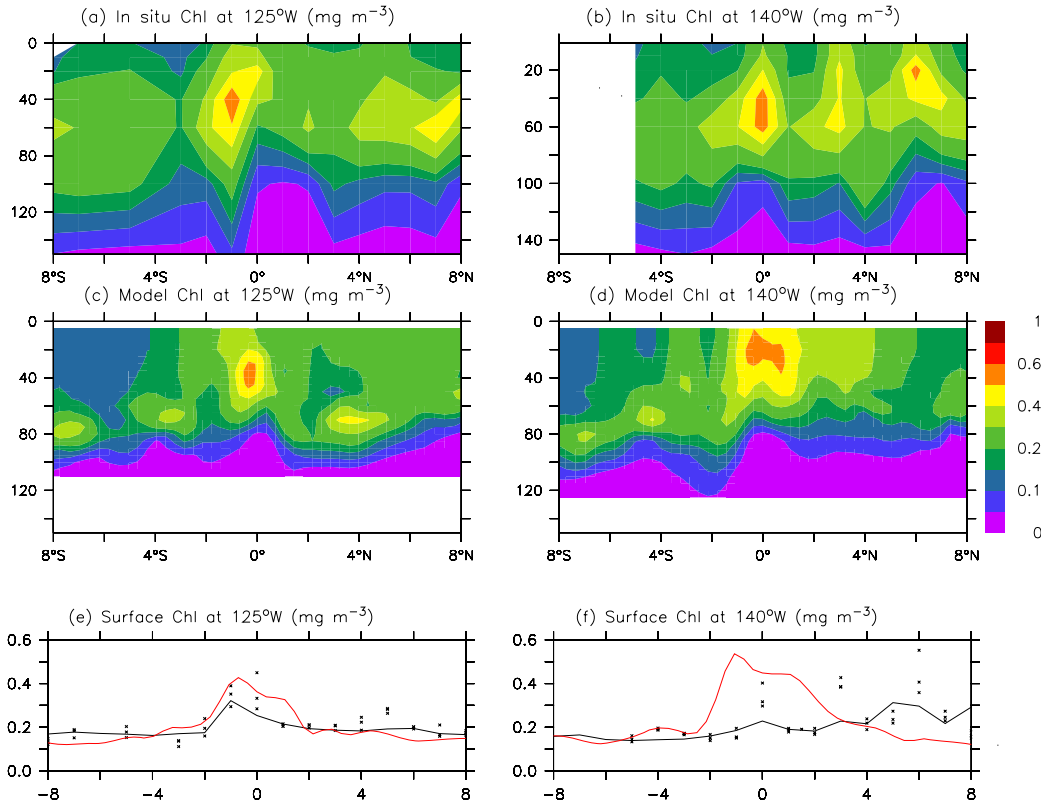

Fig. 6. SeaWiFS, in situ and modeled chlorophyll during May 2007. In situ chlorophyll **(a)** along 125° W and **(b)** along 140° W, and modeled chlorophyll **(c)** along 125° W and **(d)** along 140° W, and surface (0–20 m) chlorophyll concentrations **(e)** along 125° W and **(f)** along 140° W from in situ (symbols), model (red lines) and SeaWiFS (black lines).

BGD
5, 3869–3903, 2008

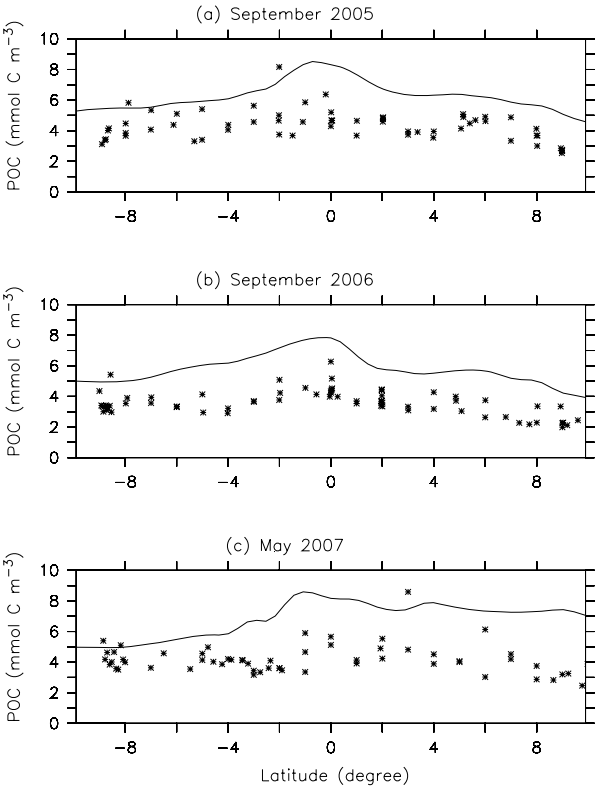

Fig. 7. Modeled (lines) versus measured (symbols) surface concentrations of POC (140° W–125° W) during **(a)** September 2005, **(b)** September 2006, and **(c)** May 2007.

BGD
5, 3869–3903, 2008

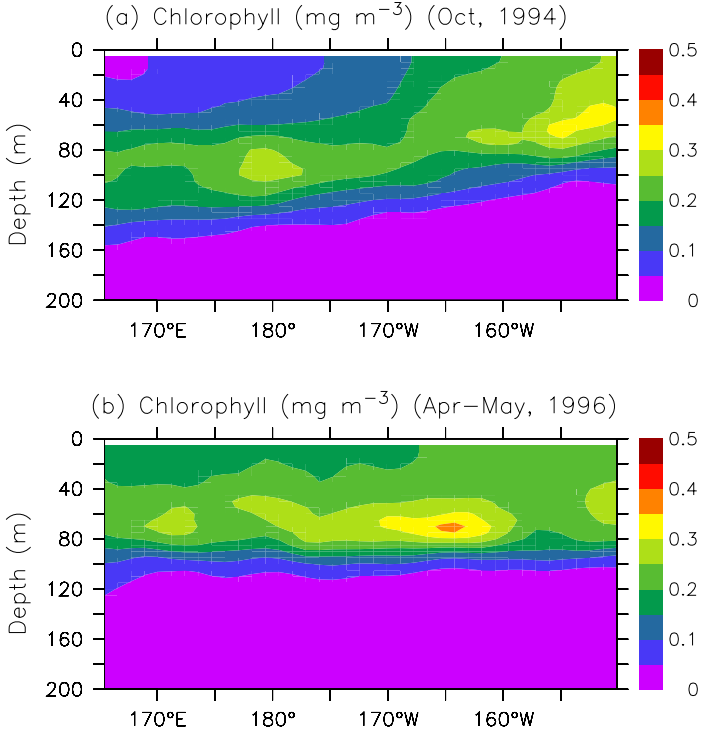

Fig. 8. Modeled zonal distributions of chlorophyll averaged over 2° N–2° S during **(a)** October 1994 and **(b)** April–May 1996.

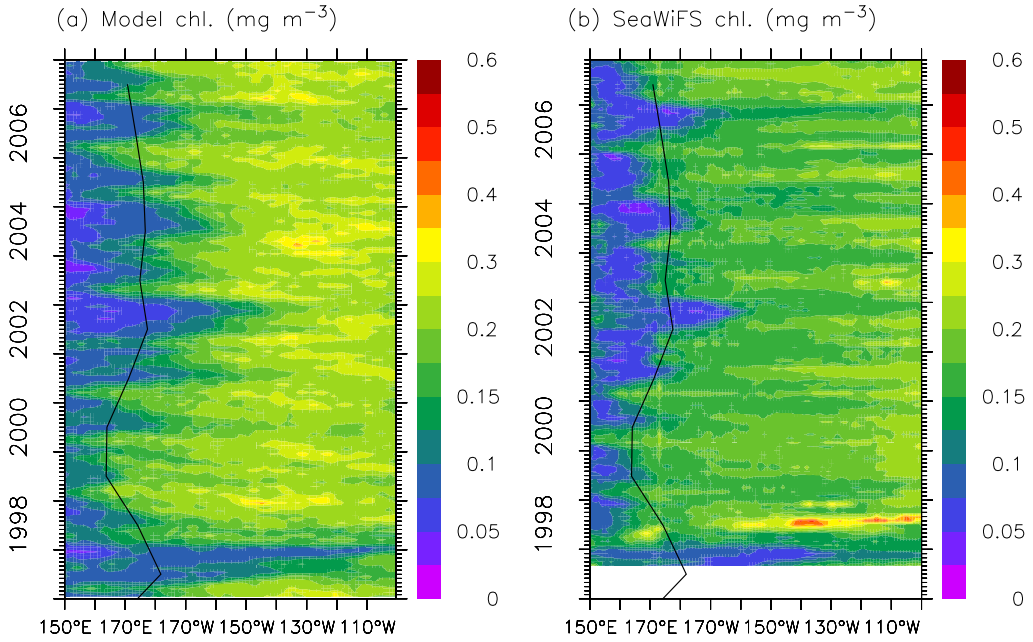

Fig. 9. Time-longitude contours of surface chlorophyll concentration (5° N–5° S) from **(a)** model and **(b)** SeaWiFS. The black lines denote the HNLC front.

BGD
5, 3869–3903, 2008

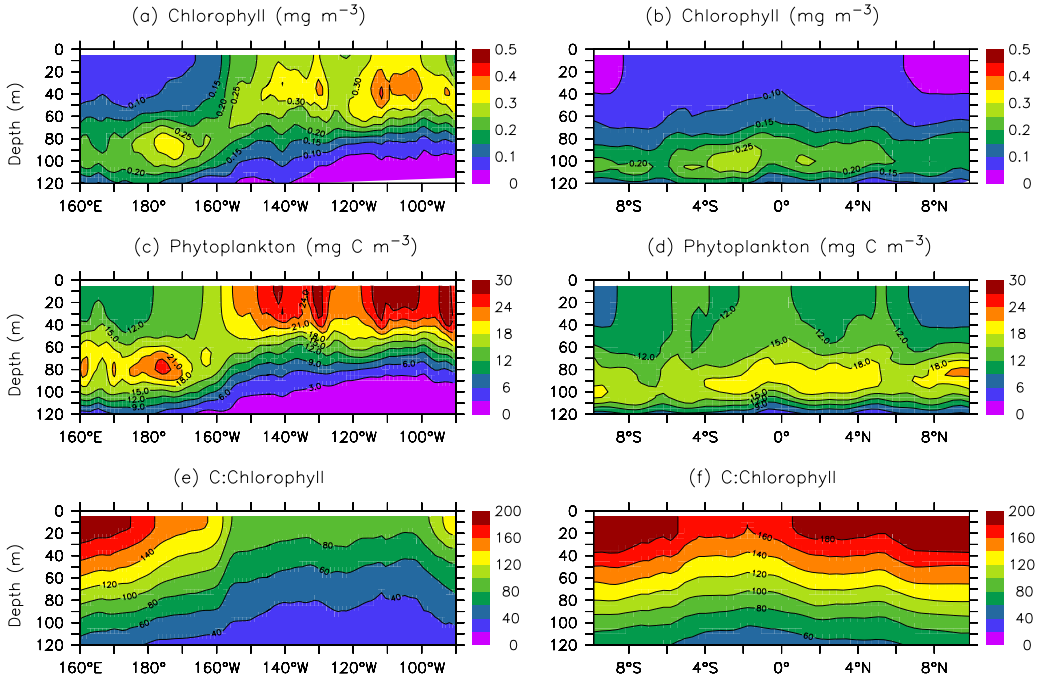

Fig. 10. Profiles of **(a)** and **(b)** chlorophyll, **(c)** and **(d)** phytoplankton carbon biomass, and **(e)** and **(f)** phytoplankton C:Chl ratio along the equator (2° N–2° S) (left panels) and along 165° E (right panels) during September–October 1994 from the standard simulation.

BGD
5, 3869–3903, 2008

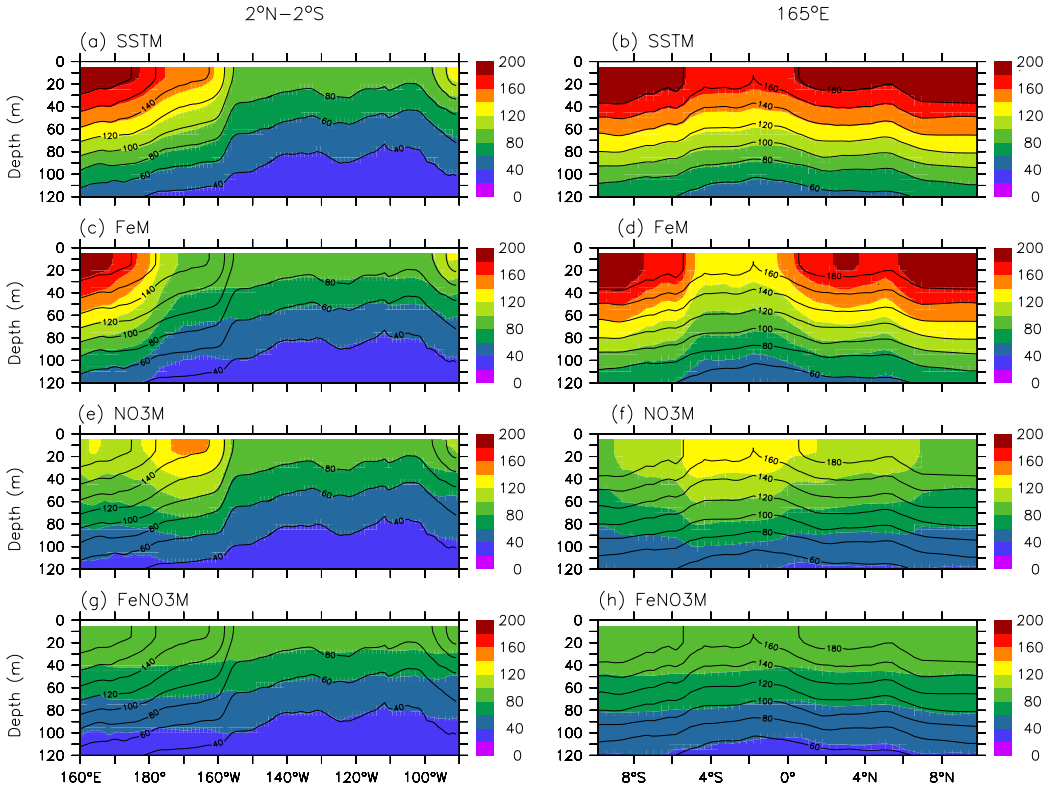

Fig. 11. Profiles of the phytoplankton C:Chl ratio along the equator (2° N–2° S) (left panels) and along 165° E (right panels) during September–October 1994 from **(a)** and **(b)** the SSTM, **(c)** and **(d)** the FeM, **(e)** and **(f)** the NO_3M, and **(g)** and **(h)** the $FeNO_3M$. Superimposed black lines are from the standard simulation.

BGD
5, 3869–3903, 2008